CONF-800804--9

LA-UR - 80 - 75

TITLE: A COMPUTATIONAL METHOD FOR FREE SURFACE HYDRODYNAMICS

AUTHOR(S): C. W. Hirt and B. D. Nichols

SUBMITTED TO: ASME 1980 Pressure Vessels and Piping Conference
August 12-15, 1980
St. Francis Hotel, San Francisco, CA

University of California

LOS ALAMOS SCIENTIFIC LABORATORY
Post Office Box 1663 Los Alamos, New Mexico 87545
An Affirmative Action/Equal Opportunity Employer

Form No. 836 R3
St. No. 2629
12/78

UNITED STATES
DEPARTMENT OF ENERGY
CONTRACT W 7405-ENG 36

A COMPUTATIONAL METHOD FOR FREE SURFACE HYDRODYNAMICS

C. W. Hirt and B. D. Nichols
Theoretical Division, Group T-3
University of California
Los Alamos Scientific Laboratory
Los Alamos, NM 87545

ABSTRACT

There are numerous flow phenomena in pressure vessel and piping systems that involve the dynamics of free fluid surfaces. For example, fluid interfaces must be considered during the draining or filling of tanks, in the formation and collapse of vapor bubbles, and in seismically shaken vessels that are partially filled. To aid in the analysis of these types of flow phenomena, a new technique has been developed for the computation of complicated free-surface motions. This technique is based on the concept of a local average volume of fluid (VOF) and is embodied in a computer program for two-dimensional, transient fluid flow called SOLA-VOF. The basic approach used in the VOF technique is briefly described, and compared to other free-surface methods. Specific capabilities of the SOLA-VOF program are illustrated by generic examples of bubble growth and collapse, flows of immiscible fluid mixtures, and the confinement of spilled liquids.

I. INTRODUCTION

Numerical simulations of fluid flows undergoing large deformations are most easily performed using Eulerian representations for the flow variables. That is, the flow is computed relative to a grid of small control volumes that remain fixed in space. However, where free surfaces or other free boundaries are present, special techniques must be devised to track these surfaces in the Eulerian grid. The need for a special treatment can be readily understood from the following argument. After one time step of calculation all fluid elements that find themselves in a given cell of the grid must be averaged together to define cell values needed for the next time step. This averaging procedure introduces a smoothing of all variations in the flow variables. In particular, surfaces of discontinuity such as free surfaces can be smoothed to the point of being unrecognizable.

To overcome the numerical smoothing of interfaces a special interface tracking method is needed that satisfies three basic requirements. First, it must provide a numerical description of the location and shape of the boundary. Second, there must be an algorithm for advancing the boundary description in time. Finally, a scheme must be provided for imposing the desired boundary conditions on fluid in the surrounding computational grid.

A variety of interface tracking methods satisfying the above requirements are available, but most have limitations of one sort or another. For example, the definition of a surface by its height above some reference level ($y = h(x,t)$ in two dimensions) is a simple definition requiring a minimum of stored information, but it is limited to single-valued surfaces.

Lagrangian marker particles linked together by straight line segments can be used to define (in two dimensions) arbitrary surfaces. The disadvantage of this method is that the intersection of surfaces becomes a difficult computational problem and such intersections are usually allowed only with special, problem dependent, logic statements. Alternatively, marker particles can be used to mark all fluid-occupied regions rather than the boundaries of the regions. In this way the intersection of surfaces is no problem. Unfortunately, this method needs considerably more storage and computational time than the other methods because it requires several marker particles in each cell occupied by fluid and each particle must be moved every time step. To determine where a boundary is located also requires keeping track of all particles in a cell so that an average surface location can be computed.

In this paper another method is described that is simple and yet incorporates all the desirable features of the other methods. This new method, referred to as the volume of fluid (VOF) method, is based on a function whose value is unity at any point occupied by fluid and zero elsewhere. The average value of this function, F, in a grid cell then represents the fractional volume of the cell occupied by fluid. Thus, a unit value of F indicates the cell is full of fluid, while a zero value indicates an empty cell. Cells with F values between zero and one must then contain a boundary. Computer storage for the VOF method is a minimum at one word per cell, which is equivalent to the storage requirement for all other flow variables. Because it follows fluid regions rather than surfaces it also works for arbitrarily intersecting surfaces. In addition, the F distribu-

tion used in the VOF method has all the remaining properties desired of an interface tracking scheme. Surface locations, slopes, and curvatures are easily computed for the setting of boundary conditions, and the F distribution can be advanced in time by advection through the Eulerian grid. However, to avoid the type of numerical smoothing noted earlier it is necessary to use special advection algorithms. In the SOLA-VOF program, described in the next section, a type of donor-acceptor fluxing is used to compute the advection of F. This technique is simple and works quite well for most applications.

The VOF-based program, SOLA-VOF, that is described in Sec. II is a general purpose solution algorithm for a wide class of fluid dynamics problems. Originally the program was developed to solve time-dependent problems involving an incompressible Navier-Stokes fluid containing free surfaces. In its present form, however, SOLA-VOF is also applicable to problems involving two immiscible fluids. Additionally, it has an option for including surface tension with wall adhesion, an option for limited compressibility effects, and it has an internal obstacle capability. SOLA-VOF is an easy to use program because of numerous automatic features. For example, it has a flexible grid generator, built-in time step controls, and some self-testing features that automatically detect numerical stability problems and correct them.

A variety of sample calculations illustrating the power and usefulness of the SOLA-VOF program are presented in Sec. III. These examples cover a wide range of fluid phenomena associated with pressure vessels and piping systems.

II. THE SOLA-VOF PROGRAM

The governing differential equations are the Navier-Stokes momentum equations [1],

$$\frac{\partial u}{\partial t} + u \frac{\partial u}{\partial x} + v \frac{\partial u}{\partial y} = - \frac{1}{\rho} \frac{\partial p}{\partial x} + g_x + \nu \left[\frac{\partial^2 u}{\partial x^2} + \frac{\partial^2 u}{\partial y^2} + \xi \left(\frac{1}{x} \frac{\partial u}{\partial x} - \frac{u}{x^2} \right) \right]$$

$$\frac{\partial v}{\partial t} + u \frac{\partial v}{\partial x} + v \frac{\partial v}{\partial y} = - \frac{1}{\rho} \frac{\partial p}{\partial y} + g_y + \nu \left[\frac{\partial^2 v}{\partial x^2} + \frac{\partial^2 v}{\partial y^2} + \frac{\xi}{x} \frac{\partial v}{\partial x} \right] . \qquad (1)$$

Fluid pressure is here denoted by p. Velocity components (u,v) are in the Cartesian coordinate directions (x,y) or axisymmetric coordinate directions (r,z). The choice of coordinate system is controlled by the value of ξ, where $\xi = 0$ corresponds to Cartesian and $\xi = 1$ to axisymmetric geometry. Body accelerations are denoted by (g_x, g_y), ν is the coefficient of kinematic viscosity, and ρ is the fluid density.

If the fluid is to have limited compressibility the appropriate mass continuity equation is [2]

$$\frac{1}{\rho C^2} \frac{\partial p}{\partial t} + \frac{\partial u}{\partial x} + \frac{\partial v}{\partial y} + \frac{\xi u}{x} = 0 \qquad (2)$$

where C is the adiabatic speed of sound in the fluid. For incompressible fluids $1/C^2$ is set to zero. In the limited compressibility model density changes are assumed to be small (say less than 10%) and the ρ appearing in the pressure gradient terms in Eq. (1) can be treated as constant. [When two immiscible fluids are present this ρ is an appropriate local mixture of the constant ρ values for each fluid.]

Equations (1) and (2) are discretized with respect to an Eulerian grid of fixed rectangular cells. Grid cells may have variable sizes, say δx_i for the ith column and δy_j for the jth row, as shown schematically in Fig. 1. Dependent variables are located at the staggered grid locations indicated for a typical cell in Fig. 2.

The basic procedure for advancing a solution through one increment in time, t, consists of three steps:

(1) Explicit finite difference approximations of Eq. (1) are used to compute first guesses for the new time-level velocities. In this step the initial dependent variable values, or the values from the previous time-level, are used to evaluate all advective, pressure, and viscous accelerations.

(2) To satisfy the continuity equation, Eq. (2), pressures are iteratively adjusted in each cell. As each pressure value is changed the velocities dependent on this pressure are also changed. This pressure iteration is continued until Eq. (2) is satisfied to a prespecified level of accuracy.

(3) Finally, the F function defining fluid regions is updated to give the new fluid configuration. After all necessary bookkeeping adjustments are completed, including data output, this three-step process can be restarted for the next time-level calculation. At each step, of course, suitable boundary conditions must be imposed at all boundaries.

The actual finite difference approximations used in SOLA-VOF for Eqs. (1) and (2) are not a crucial part of the algorithm. That is, various approximations could be used without affecting the basic solution procedure.

The reader is referred to Refs. [3,4] for the particular approximations used in the present program. This flexibility does not apply, however, to the way in which the F distribution is advanced in time. Because F is a scalar quantity fixed in the fluid its evolution is governed by pure advection,

$$\frac{\partial F}{\partial t} + \frac{1}{r}\frac{\partial rFu}{\partial x} + \frac{\partial Fv}{\partial y} = 0 \quad , \tag{3}$$

where $r = x$ when $\xi = 1$ and $r = 1$ when $\xi = 0$. This equation is strictly valid only for incompressible flow, but is also acceptable for the limited compressibility approximation. Numerical approximations to Eq. (3) must be constructed with special care to avoid numerical smoothing of the F distribution. There are several ways to do this. SOLA-VOF employs a type of donor-acceptor fluxing using the fact that F values should be either one or zero. The basic idea can be grasped by considering the amount of F to be fluxed across the right boundary of a cell during one time step. The total volume of both fluid and void crossing the boundary, per unit cross-sectional area, is $V = u\delta t$, where u is the normal velocity at the boundary. The sign of u determines which cell is losing F (the donor) and which is gaining F (the acceptor). The amount of F crossing the boundary depends on how F is distributed in the donor cell. When the flux is primarily in the direction normal to the F surface the fractional area of the flux boundary across which F is flowing is determined by the acceptor cell F value. When the flux is primarily tangent to the surface the donor cell F value is used. In both cases the amount of F fluxed is computed as the product of the cross-sectional area of the flux boundary times δF where,

$$F = \text{MIN}\{F_{AD}|V| + CF \ , \ F_D \ \delta x_D\}$$

and where

$$CF = \text{MAX}\{(1.0 - F_{AD})|V| - (1.0 - F_D)\ \delta x_D \ , \ 0.0\} \quad . \qquad (4)$$

Subscripts denote acceptor (A) and donor (D) cell values. The double subscript (AD) is equal to A when the flux is normal to the free boundary and equal to D otherwise. The MIN feature in Eq. (4) prevents more F being fluxed than is available in the donor cell. The MAX feature accounts for an additional flux of F if more than the amount of void volume available in the donor cell is fluxed. Figure 3 illustrates these features for several typical cases. The fluid is assumed distributed in the donor and acceptor cells as shown depending on the orientation of the surface normal with respect to the flux direction. In Fig. 3a the donor cell, acceptor cell, and the flux volume are defined. Then Fig. 3b illustrates a situation in which the donor cell value of F is used to define the fractional area of the flux boundary open for fluxing F. In case c of Fig. 3 the acceptor cell value of F has been used to define the fractional area. In this case all the F region in the donor cell is fluxed, but it is less than the total flux possible, which illustrates the use of the MIN test in Eq. (4). Finally, in Fig. 3d, more F than the amount determined by the acceptor cell defined area must be fluxed. The extra flux contribution to F is the quantity CF defined in Eq. (4).

The choice of the acceptor or donor cell F value to define a flux area, which depends on the orientation of the free boundary, is a feature not used in other schemes of this type. It is essential to do this, however, otherwise boundaries advecting more or less parallel to themselves will develop step irregularities.

Additional details of the SOLA-VOF program relating to boundary conditions, numerical stability requirements, etc., can be found in Refs. [3,4].

The best way to assess the strengths and weaknesses of the SOLA-VOF algorithm is to examine the calculations it can perform. This is done in the next section, where several applications are used to illustrate its power for a wide variety of difficult problems.

III. SAMPLE APPLICATIONS

Pressure vessels and piping systems are subject to many kinds of complex flow phenomena. The following examples have been chosen to illustrate how some of these phenomena can be addressed with the new SOLA-VOF program. These examples cover problems involving the growth and collapse of vapor bubbles, problems associated with mixtures of immiscible fluids, and problems involving extreme deformations of free surface dominated flows.

A. Bubble Dynamics

In pressurized systems for liquid transport it is sometimes possible for vapor bubbles to form. Under most circumstances bubbles are undesirable as their growth or collapse can result in significant pressure fluctuations and local material damage. The theoretical prediction of bubble dynamics is complicated by the generally large free surface deformations involved. This, then, is an excellent area where the capabilities of the

SOLA-VOF program can be put to use. For purposes of illustration we shall consider what happens when steam is forced through a pipe submerged in a pool of water. The pipe is located axisymmetrically in a cylindrical vessel approximately half filled with water (see Fig. 3). Experimental studies [5] indicate that when sufficient steam is injected into the pipe bubbles may repeatedly form and collapse at the end of the pipe causing large pressure transients to be generated in the water pool. Presumably the increase in liquid surface area and stirring associated with the formation of a bubble increases the condensation of steam to the point where it can no longer support the bubble. When this happens the bubble collapses and water rushes back into the pipe until sufficient steam pressure is again built up to generate a new bubble.

To simplify the problem we shall not attempt to model all the processes associated with actual steam condensation, but shall use a simple prescribed pressure history for the steam. In particular, the steam pressure is approximately linearly increased until a bubble has been generated then it is rapidly reduced to the saturation pressure of the water in the pool. A one millisecond time interval was arbitrarily chosen for the depressurization time. The time at which the depressurization is started determines the size of the bubble transient. This crude model approximates what would happen with a more detailed condensation model in which condensation proceeds more rapidly than the inertial response time for the bubble. In any case, it is sufficient to illustrate how the SOLA-VOF program can be used to study the complete history of bubble birth and death.

Starting from an initial vapor pressure of 1.1 psia in the pipe (0.146 ft I.D.) the pressure is increased to about 3.16 psia over a period of 190 ms then is ramped down in 1 ms to 0.38 psia. A sequence of computed velocity plots and fluid configurations are shown in Fig. 4. The earliest time shown corresponds to the time at which the vapor pressure is ramped down to the liquid saturation pressure. Because of inertia in the liquid the bubble continues to grow (Fig. 4c). When the bubble begins to collapse it does so asymmetrically, pulling liquid in from the top of the pool. This causes a detached bubble to form shortly after Fig. 4d, which then disappears some time between Figs. 4e and 4f. Water is seen to be moving rapidly up the pipe in the final frame.

Pressures computed at the center of the vessel floor are shown in Fig. 5. The initial rapid increase in floor pressure occurs shortly after the pipe has been cleared of water. At 0.19 s the pressure drops because of the decrease in vapor pressure at that time. A relatively violent pressure transient develops when water reenters the pipe end and the detached bubble collapses. This transient, denoted by the dashed line in Fig. 5, is shown in an expanded scale in Fig. 6. To obtain this result the fluid must be treated as a compressible medium because the pressure transients have characteristic times short compared to the time needed for acoustic waves to travel across the pool. Except for this short, violent transient the water can be treated as incompressible, but to correctly estimate the pressure pulse generated by the final bubble collapse requires compressibility. The limited compressibility model available in the SOLA-VOF program provides this capability.

B. Immiscible Fluids

A mixture of oil and water provides an excellent example of a two-fluid system often encountered in practical situations. Because of their slightly differing densities and the action of interfacial surface tension forces the mixture behaves dynamically quite different than either fluid separately.

Using the two fluid and surface tension options in the SOLA-VOF program a variety of interesting mixture problems can be investigated. To illustrate, Fig. 7 presents results from a calculation of the passage of a liquid drop through a constriction in a tube. The drop has a density equal to 9/10 of the density of the surrounding fluid. Surface tension at the interface between the two fluids is such that the Weber number ($\rho V^2 r/\sigma$) is equal to 0.192, based on the drop radius and average flow rate through the tube. This means that surface tension forces are more significant than those of inertia. In this example viscous forces are also relatively strong for the Reynolds number (Vr/ν) was chosen to be 1.25, and it was assumed that both fluids have the same kinematic viscosity. Flow entering the flow channel is uniform, implying that the constriction is near the channel entrance where boundary layers have had little time to develop. If this were an oil-water mixture, it would correspond to a small oil drop ($r = 3 \times 10^{-4}$ cm) forced rapidly ($V = 46.1$ cm/s) through a hole in a thin plate.

To force the drop through the constriction requires extra work to deform the drop against its surface tension forces, Figs. 7a-7c. Much of this work, however, is recovered as the drop emerges from the constriction, Figs. 7d-7f.

C. Large Distortion Dynamics

The advantage of formulating SOLA-VOF in terms of an Eulerian representation is its ability to treat flows undergoing extreme deformations. To illustrate this capability consider what happens when a tank containing fluid collapses. Suppose a dike is to be constructed around the tank to contain the spilled fluid. The problem is how high to build the dike. A specific example is illustrated in Fig. 8. The fluid is initially a circular column having a height equal to its diameter. The dike is a low axisymmetric wall whose radius has been arbitrarily chosen to be $2\frac{1}{2}$ column radii. As the column collapses fluid rushes radially outward along the ground. Upon striking the dike the leading edge of the fluid is deflected upward, but if the dike isn't high enough it retains sufficient radial momentum to splash down outside the dike. This is seen to be the situation in Fig. 8 where a significant amount of fluid has been lost from the dike region. When the dike height is increased to approximately 2 times the height shown in Fig. 8, additional calculations indicate that virtually all the fluid is contained within the dike.

Although this is a conceptually simple problem, it is obviously one that involves highly complicated free surface dynamics. Nevertheless, the SOLA-VOF program does a remarkable job in representing the flow. Other variations involving different initial fluid and obstacle configurations are easily imagined. Of course, SOLA-VOF could also be used for similar problems involving two immiscible fluids with or without interfacial surface tension. It is this flexibility, in fact, that makes the SOLA-VOF program such a powerful tool. With thoughtful use it provides a means of investigating many previously intractable problems associated with pressurized fluid systems.

ACKNOWLEDGMENTS

We wish to thank R. S. Hotchkiss for his efforts in adding the surface tension capability to the SOLA-VOF program and for running the second example problem. This work was supported by the Electric Power Research Institute under contract RP-965-3.

REFERENCES

1. L. D. Landau and E. M. Lifshitz, Fluid Mechanics, Pergamon Press, London, 1959.

2. C. W. Hirt and B. D. Nichols, "Adding Limited Compressibility to Incompressible Hydrocodes," J. Comp. Phys. 33, 1979.

3. C. W. Hirt and B. D. Nichols, "Volume of Fluid (VOF) Method for the Dynamics of Free Boundaries," submitted to J. Comp. Phys., 1979.

4. B. D. Nichols, C. W. Hirt, and R. S. Hotchkiss, "SOLA-VOF: A Solution Algorithm for Transient Fluid Flow with Multiple Free Boundaries," Los Alamos Scientific Laboratory report in preparation.

5. G. B. Andeen and J. S. Marks, "Analysis and Testing of Steam Chugging in Pressure Systems," Electric Power Research Institute report NP-908, 1978.

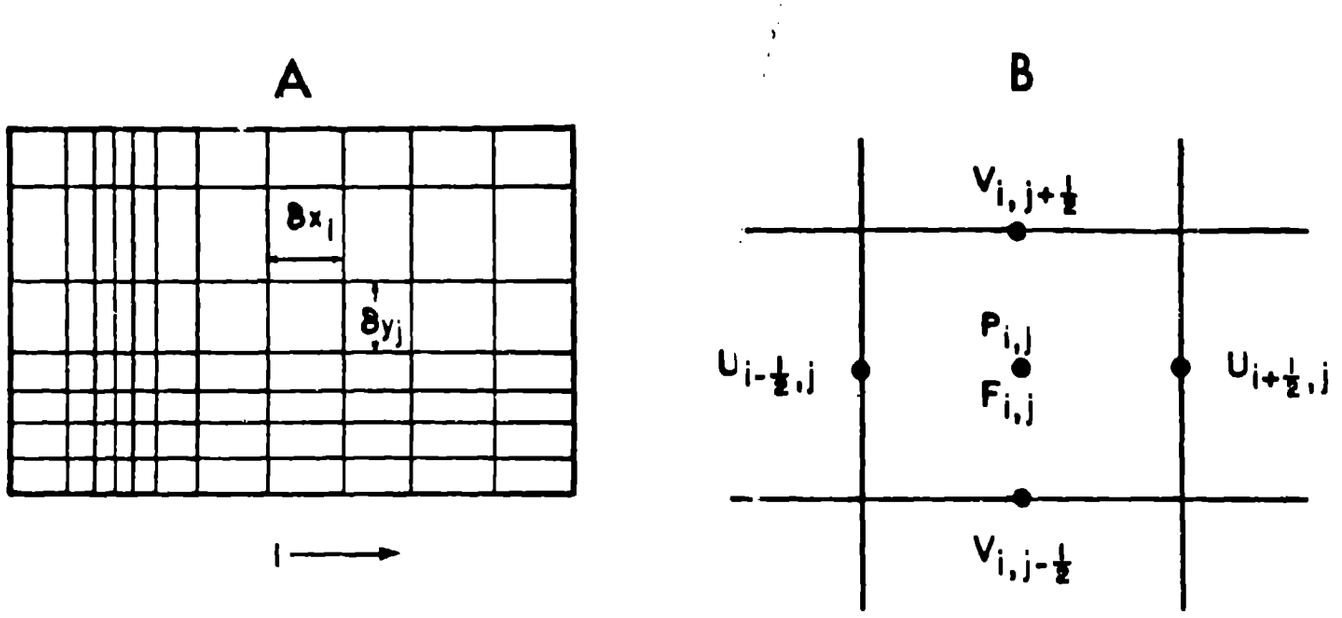

Fig. 1. (A) Mesh setup showing variable cell capability. (B) Location of dependent variables in a typical mesh cell.

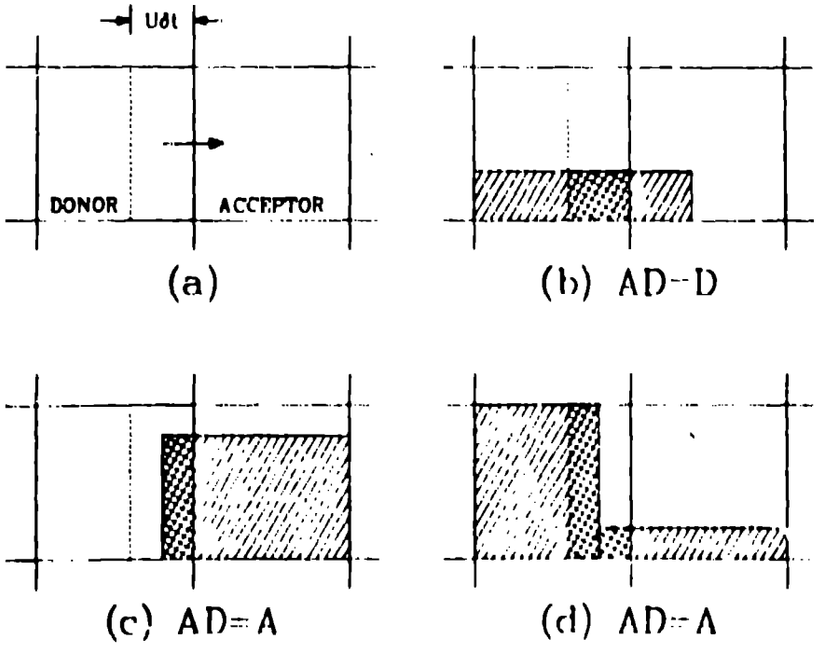

Fig. 2. Schematic used in calculating F advection. Donor-acceptor cells are defined in (a) where dashed line indicates left side of flux volume. Cross-hatched regions in (b-d) are the amounts of F advected.

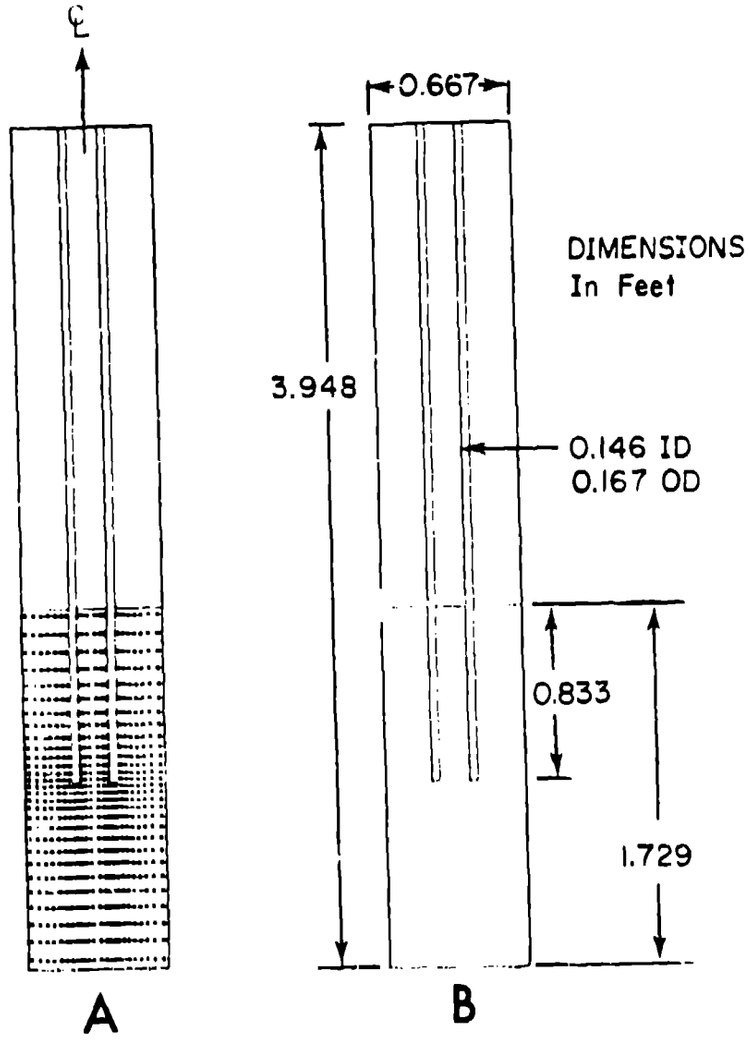

Fig. 3. Schematic of steam injection apparatus used by SRI International. Plus signs in (a) indicate mesh cell centers that initially contain fluid. Dimensions of apparatus are shown in (b).

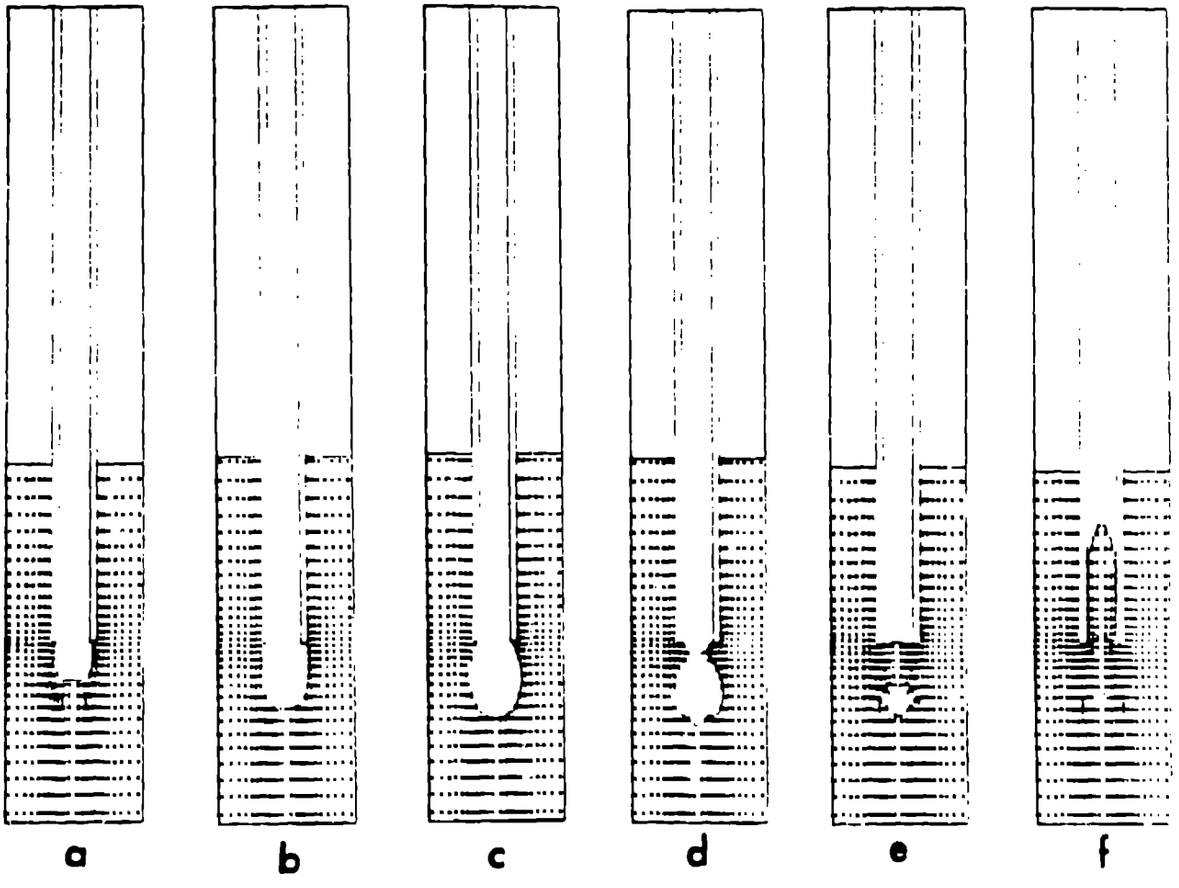

Fig. 4. Velocity vectors and fluid configurations at selected times after initiation of pressurization. Times in seconds are (a) 0.19, (b) 0.21, (c) 0.22, (d) 0.24, (e) 0.25, and (f) 0.30.

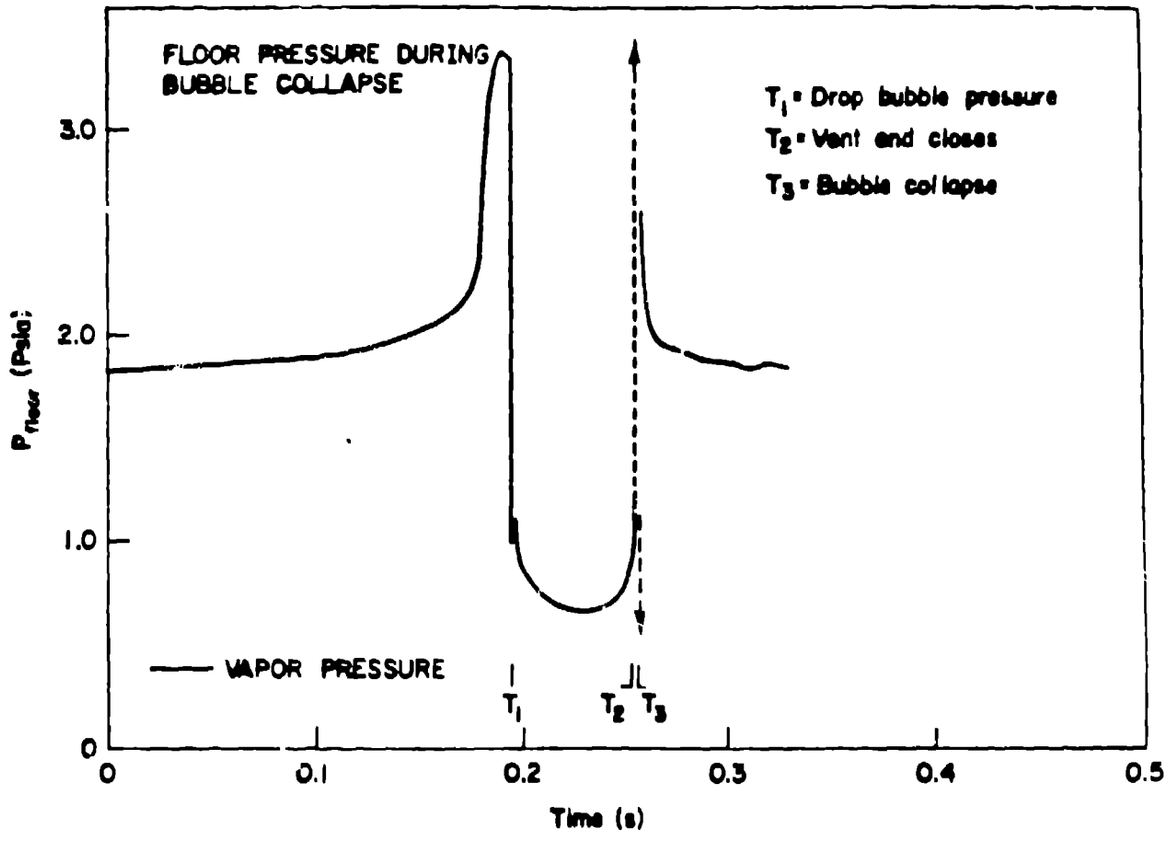

Fig. 5. Floor pressure history computed during bubble growth and collapse. Dashed line region shown in expanded time scale in Fig. 6.

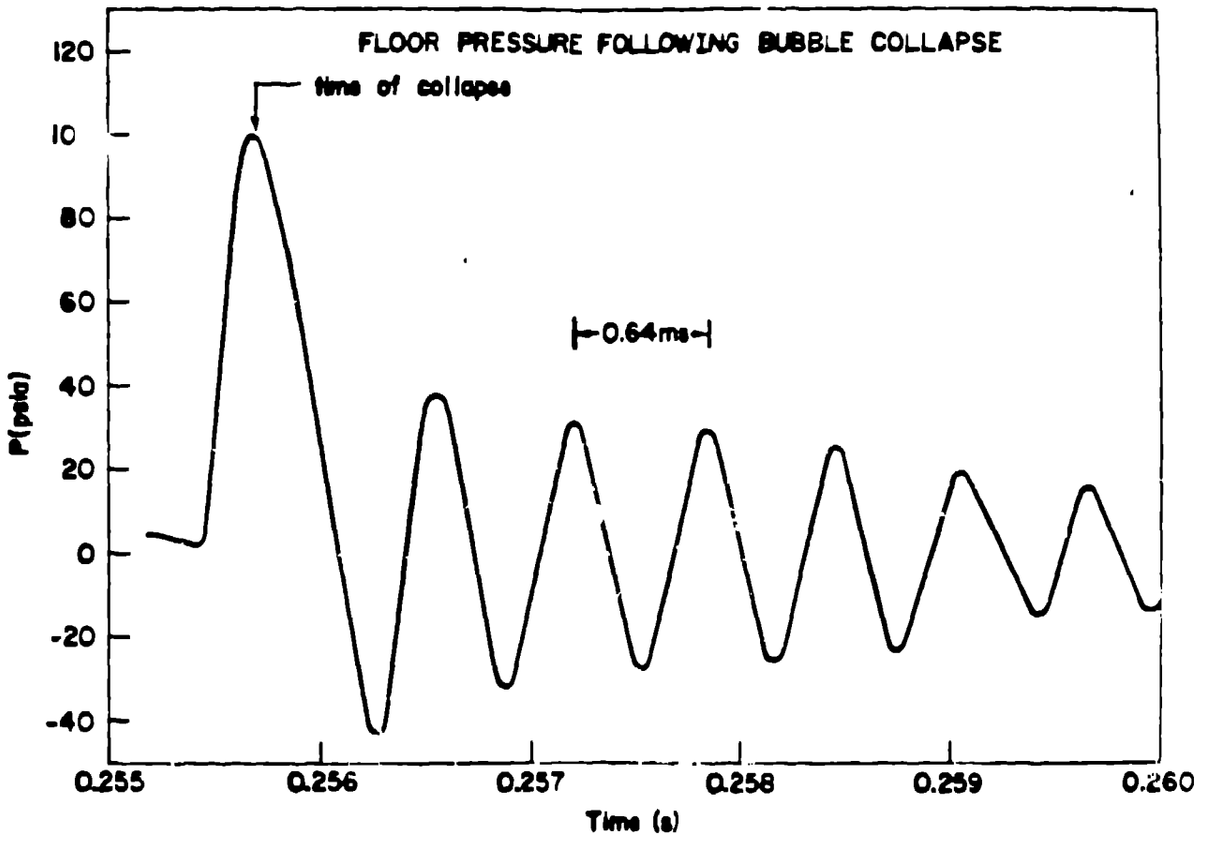

Fig. 6. Computed floor pressure on an expanded time scale following bubble collapse.

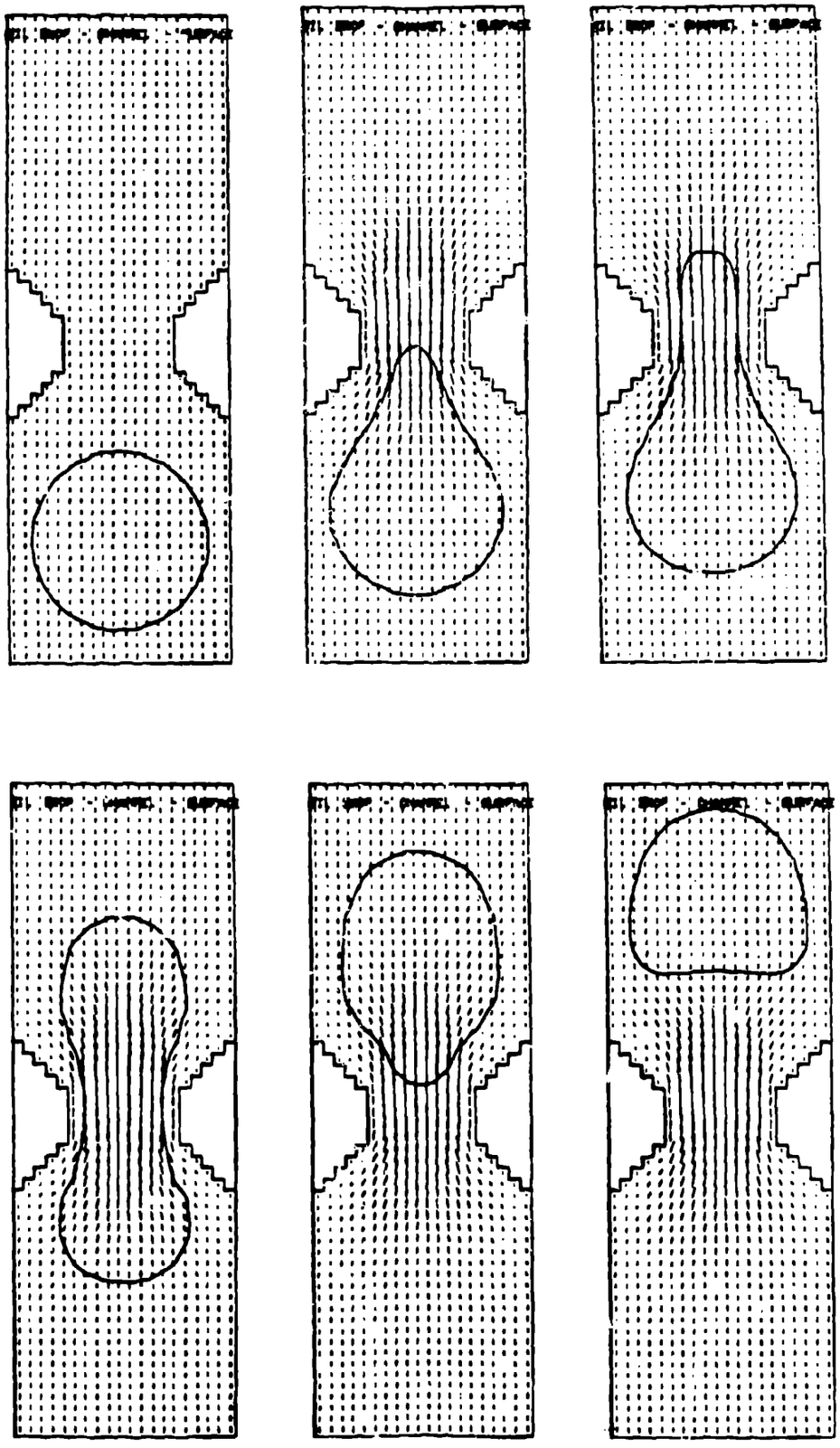

Fig. 7. Distortion of an immiscible fluid drop passing through a constriction.

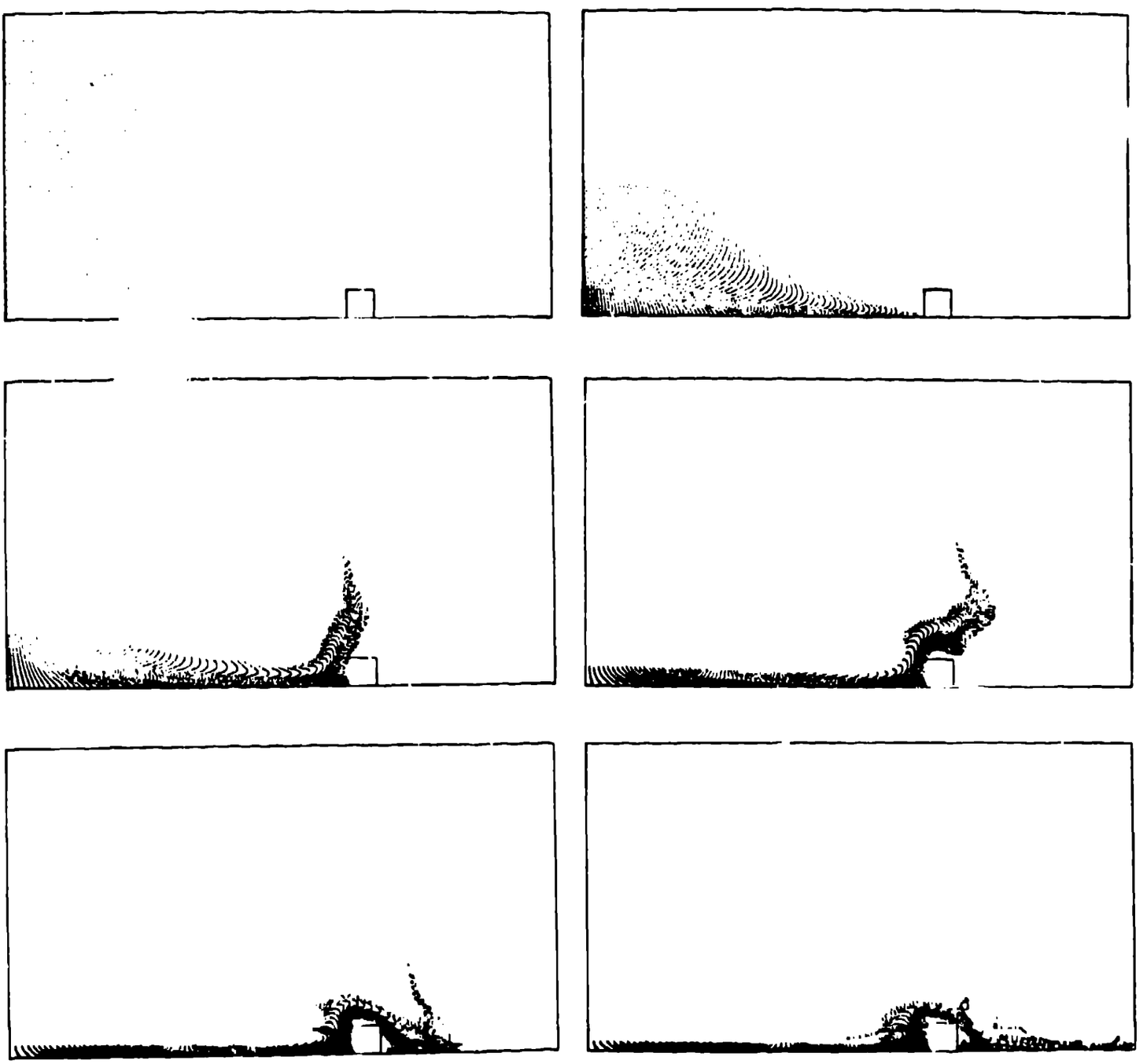

Fig. 8. Collapse of a cylindrical column of fluid and its partial confinement by a low dike. Cylindrical axis is at left edge of figures.